analytical chemistry

ARTICLE

pubs.acs.org/ac

Time-Gated Luminescence Microscopy Allowing Direct Visual Inspection of Lanthanide-Stained Microorganisms in Background-Free Condition

Dayong Jin* and James A. Piper

Advanced Cytometry Laboratories at Macquarie, MQ Biofocus Research Centre, Faculty of Science, Macquarie University, NSW 2109 Australia

Supporting Information

ABSTRACT: Application of standard immuno-fluorescence microscopy techniques for detection of rare-event microorganisms in dirty samples is severely limited by autofluorescence of nontarget organisms or other debris. Time-gated detection using gateable array detectors in combination with microsecond-lifetime luminescent bioprobes (usually lanthanide-based) is highly effective in suppression of (nanosecond-lifetime) autofluorescence background; however, the complexity and cost of the instrumentation is a major barrier to application of these techniques to routine diagnostics. We report a practical, low-cost implementation of time-gated luminescence detection in a standard epifluorescence microscope which has been modified to include a high-power pulsed UV light-emitting diode (LED) illumination source and a standard fast chopper inserted in the focal plane behind a microscope eyepiece. Synchronization of the pulsed illumination/gated detection cycle is driven from the clock signal from the chopper. To achieve time-gated luminescence intensities sufficient for direct visual observation, we use high cycle rates, up to 2.5 kHz, taking advantage of the fast switching capabilities of the LED source. We have demonstrated real-time direct-visual inspection of europium-labeled *Giardia lamblia* cysts in dirty samples and *Cryptosporidium parvum* oocysts in fruit juice concentrate. The signal-to-background ratio has been enhanced by a factor of 18 in time-gated mode. The availability of low-cost, robust time-gated microscopes will aid development of long-lifetime luminescence bioprobes and accelerate their application in routine laboratory diagnostics.

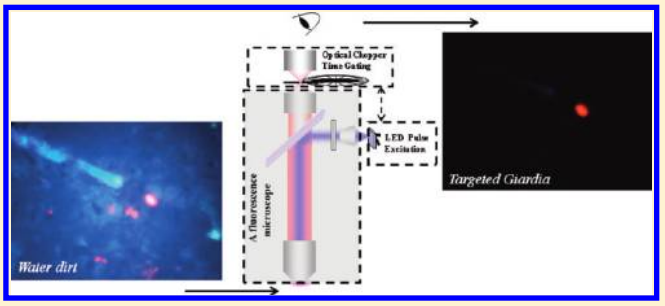

Standard fluorescence microscopy techniques are based on spatial variation of emission intensity within specific wavelength bands which are characteristic of target (e.g., immunofluorescence-labeled) organisms or cellular fractions. However, for applications such as rare-event detection (1 target cell in $>10^5$ nontarget background microorganisms),[1,2] immunocytochemistry or intracellular assays,[3] standard fluorescence microscopy suffers a key drawback affecting both visual and electronic detection sensitivity, notably the existence of strong autofluorescence from nontarget elements in wavelength bands which overlap spectrally with the fluorescence or luminescence label. Water/food safety inspection serves as one typical example: due to the very small number of organisms capable of infection, the methods of analysis must be sufficiently sensitive to detect less than 10 single microorganisms (e.g., *Cryptosporidium parvum* and *Giardia lamblia*) from a matrix of concentrates from 10 L of water containing millions of nontarget microorganisms and particles.[4] One very successful approach to solving this problem, at least in the case of electronic detection, is to use pulsed excitation and time-gated detection in combination with luminescent probes with comparatively long emission lifetimes, to effectively discriminate against the short-lifetime signal of autoflourescence (Figure 1).

The use of lanthanide-based luminescence probes (characterized by emission lifetimes $10^{-4}-10^{-3}$ s and narrow emission spectra ~10 nm[5−7]) for time-gated luminescence (TGL) detection was first suggested in 1976,[8] and the first bioassays applying lanthanide-TGL in immunodiagnostics were reported in 1979.[9−11] TGL techniques have subsequently become a favored method in ultrahigh-contrast biosensing including immunoassay,[12−15] DNA assay,[16] high-contrast microscopy bioimaging,[17−21] and rare-event flow cytometry.[2,22,23] Recent developments of highly luminescent lanthanide complexes,[3,24,25] responsive lanthanide-based luminescent probes,[26−28] functionalized lanthanide-ion nanocomposites,[29] and nanoencapsulation lanthanide containing biolabels[30−33] further demonstrate the potential of lanthanide-based cellular imaging.

One practical problem, which arises from the relatively weak luminescence intensity of lanthanide probes and slow TGL cycling rates (~10^2 Hz) which apply to current gateable high-resolution planar-array detector technology,[20] is that quite lengthy (often 30 s) signal accumulation times are necessary to

Received: December 7, 2010
Accepted: January 24, 2011
Published: February 23, 2011

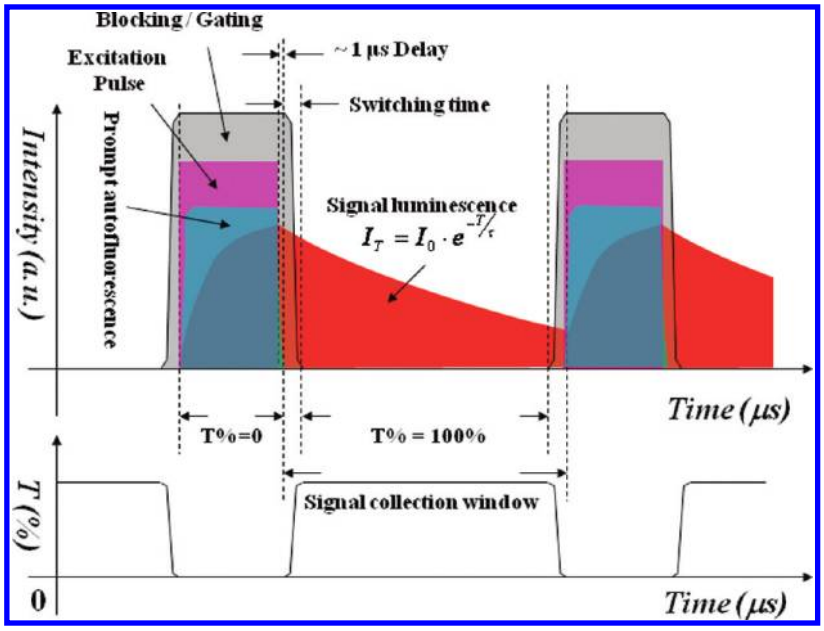

Figure 1. Schematic illustrating the principle of time-gated luminescence detection using a long-lived luminescence lanthanide bioprobe.[38]

produce quality TGL images. Thus, researchers typically report either grayscale[33,34] or pseudocolor[7,30,35] TGL cell images obtained using high-quality monochrome (high-gain CCD) cameras. A comprehensive progress review of recent developments in TGL microscopy based on lanthanide probes has been undertaken recently by Connally.[36] In the past decade, there has been a rapid evolution of the technology of TGL microscopy to make it more effective and cheaper: in the case of the pulsed excitation source, the technology has moved from chopper-interrupted continuous Hg lamps or UV lasers, to pulsed Xenon flashlamps, and most recently to current-switched UV light-emitting diodes (LEDs), and in the case of time-gated detection, the technology has evolved from mechanical chopper or ferro-electric shutter, to gated CCDs, to gated-intensifier CCDs, and most recently to gain-switched electron-multiplying CCDs.[34] Most recently, Gahlaut and Miler employed a red sensitive (photon-cathode quantum efficiency 38% at 610 nm) intensified CCD camera and successfully demonstrated the time-gated luminescence imaging of single 40 nm nanospheres (containing ~400 europium complex molecules) within 1 s acquisition times.[20] Despite these advances, TGL microscopy remains a relatively complex and expensive tool, restricting application to a small range of specialist bioassays. In 2010, Leif and Yang reported a simple analog method to electronically gate a specific monochrome-CCD camera during the charge accumulation period before reading out, which demonstrated a low-cost feasibility to realize the time-gated luminescence bioimaging.[37] In the same SPIE conference proceeding, we briefly described our preliminary results by synchronizing a UV LED as excitation to a pinhole-assisted optical chopper toward a low-cost time-gated luminescence microscope.[38] In comparison, visually scanning the luminescent slides is consistent with current practice; however, it has less sensitivity than a research grade camera (longer integration period). Simultaneous detection of multiple labels (colors) requires the use of one or more cameras and imaging paths; however, the use of an inexpensive chopper makes it reasonably economical to detect background-free luminescence with instrumentation or the human eye. To the best of our knowledge, it has been a major barrier to produce a low-cost TGL microscope allowing direct visual (naked-eye) observation of true-color TGL images in real time, such as would enable practical utilization of TGL microscopy to identify target organisms free of background in routine laboratory diagnostics.[35]

In this paper, we report the comprehensive study of the principles, evaluation, and application of real-time direct-visual observation of high-contrast lanthanide stained microorganisms in background-free condition using standard epifluorescence microscopes incorporating a comparatively simple and low-cost modification which enables time-gated operation. We believe adoption of this or similar technologies as standard options for fluorescence microscopes will open the way for application of time-gated luminescence microscopy in routine laboratory diagnostics in microbiology and pathology.

EXPERIMENTAL SECTION

Briefly, in this paper, to achieve average TGL signal intensities sufficient for direct visual observation, we implement high TGL cycle rates of 2.5×10^3 Hz using pulsed UV LED excitation and high-speed time-gating optics (a fast chopper at a pinhole at the focal plane behind the original eyepiece, refer to Figure 2) to demonstrate time-gated luminescence images with a color camera. The color information from other fluorochoromes or autofluorescence is gated out by this system.

Time gated luminescence (TGL) detection requires that target organisms are labeled with a long-lived luminescent probe, typically a lanthanide complex with a luminescence lifetime of >100 μs, more than 10 000 times longer than the autofluorescence lifetimes ($\tau < 0.01$ μs) typically associated with nontarget organisms and organic or inorganic detritus of dirty samples. Referring to Figure 1, following pulsed excitation, autofluorescence from nontarget material fades rapidly (within 0.1 μs), while target luminescence is sustained over 100s of microseconds. When fluorescence/luminescence from the sample is blocked from observation (or detection) throughout the period of illumination/excitation and for a short time delay (~1 μs) after

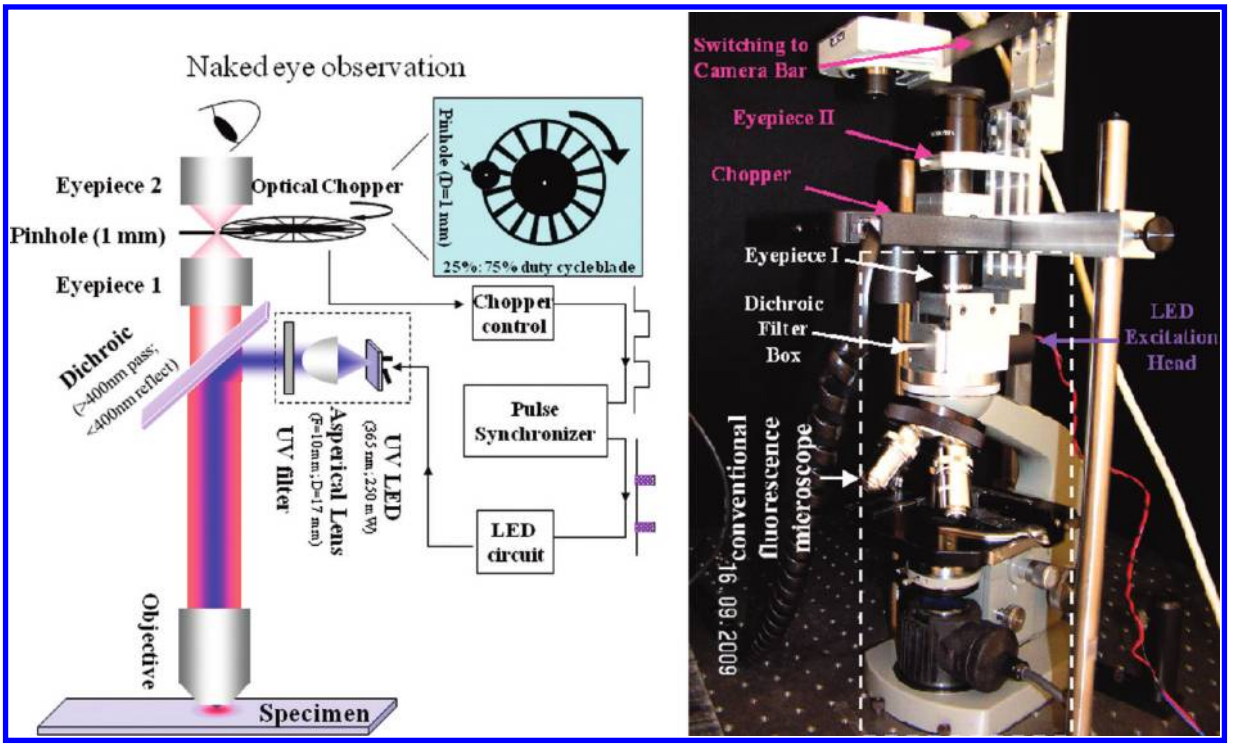

Figure 2. Left: Schematic layout of a time-gated luminescence microscope. The pulse synchronizer was referenced to the TTL signal from chopper and used to trigger the UV LED circuit, so that an appropriate time-delay between excitation pulse to gated-detection (observation) was achieved.[38,51] Right: Photograph of the prototype time-gated luminescence microscope consisting of a conventional fluorescence microscope (within the white dished box), a UV LED excitation head, an optical chopper, a second eyepiece, and a CCD camera on the switching bar.

excitation ceases, but subsequently observed during the interval between excitation pulses (the signal collection window), the signal luminescence from the target organism becomes highly distinguishable from the background autofluorescence. To achieve maximum time-gated luminescent signal, it is necessary to optimize the duty-cycle for observation (detection): this requires minimizing the illumination pulse duration consistent with maximizing the excitation and minimizing the fading of the target biolabels, minimizing the switching time between gating-off and gating-on for observation (detection) of the target luminescence, and optimizing the length of the observation (detection) period between excitation pulses consistent with the luminescence lifetime of the target biolabel.

To achieve high average TGL signal intensities sufficient for direct-visual observation using lanthanide labels, it is necessary (see Supporting Information sections S1−S4) to meet the following conditions: (1) TGL cycle rate in the range of 1−10 kHz corresponding to signal collection window 1 ms to 100 μs matching the lanthanide emission lifetime; (2) UV (~ 350 nm) pulsed excitation power $\sim 8 \times 10^{-3}$ J $[\mathrm{cm}]^{-2}$ so as to saturate the lanthanide label (Europium complex BHHCT(4,4′-bis(1″,1″,1″, 2″, 2″, 3″,3″-heptafluoro-4″, 6″-hexanedion-6″-yl)chlorosulfo-*o*-terphenyl-Eu^{3+}), see Supporting Information section S2) by the end of the excitation pulse; (3) switch-off time for the pulsed UV excitation as short as possible (<0.1 μs) with delay time to detection further delayed ~1 μs; (4) switch-on time for detection as short as possible compared with signal collection period. While switch-on times for micro-channel-plate (MCP)-gated or gain-switched CCD array detectors can be very short (submicrosecond), for direct visual inspection, the electromechanical switches (for example, fast mechanical choppers or vibrating mirrors), which might be used to implement the time-gating cycle, have much longer open-to-shut transition times, often hundreds of microseconds or more. The analog method by direct electronically shutting a CCD[37] may also provide a relatively fast switching time in a few microseconds (our preliminary experiment by switching on/off a linear array CCD resulted in a switching time of ~4 μs).

In our prototype arrangement, the current-switched UV LEDs used for the pulsed excitation source can complete the switch-on-off transition in times <3 μs and operate at cycle rates of 100s of kilohertz.[23] However, there are a limited number of options available for implementing detection-gating for visual observation. We have tested liquid crystal shutters (e.g., Oriel ferroelectric liquid crystal shutter, model 50075, http://www.newport.com/Oriel-Optical-Shutter/378983/1033/catalog.aspx), but these suffer from high optical transmission loss (typically up to 75%) and slow switching time (~80 μs) and are fragile to UV light. Vibrating choppers, such as tuning fork choppers, have been considered,[39] but their switching times are still relatively long (>50 μs), and cycle rates are low (<1 kHz).[39] Though mechanical choppers generally also have slow switching time, ~ 100−200 μs,[7,19,21,35,40,41] they have a number of advantages for the present application including 100% transparency when open and 100% blocking when closed, they provide an automatic synchronization signal (using internal optical diodes monitoring the chopper directly), and in compact forms, they can be fairly easily incorporated into microscopes. For the present demonstration, we have adopted a latest-generation compact fast chopper and a new optical configuration to achieve as short as 11 μs switching time and 2.5 kHz cycle rate, an on−off duty ratio of 3:1 (that is, 75%:25%).

Referring to Supporting Information section S1, the off-on transition time is given by $T_{switching} = D_{pinhole}/|v| = D_{pinhole}/2\pi f|r|$. It follows that maximizing both rotation rate f and the chopper blade radius ($|r|$), to give highest velocity of the chopper slots and minimizing the diameter of optical beam ($D_{pinhole}$) at the chopper slots, results in the lowest transition times. However, reducing the effective aperture of the microscope also reduces the luminescence signal from the sample. We achieve both low optical beam size at the chopper and high optical throughput by positioning the chopper next to a pinhole at the focus of the eyepiece of the microscope and then reimaging on the eye of the observer using a second eyepiece. The pinhole acts as a near-field spatial filter to determine the effective beam diameter at the chopper. This arrangement is very simple to implement both in respect of the optics and the mechanical mounting of the chopper head.

The chopper geometry and speed determine the "signal collection window" for lanthanide luminescence from the labeled (target) organisms. For the TGL microscope reported here, the signal collection window can be set to 100, 300, or 500 μs corresponding to transparent/blocking (open/closed) duty ratios 1:1, 3:1, and 5:1.

Figure 2 shows the optical layout of the time-gated luminescence microscope using the UV LED excitation. The high intensity UV LED (maximum CW output power of 250 mW at 365 nm, NCCU033A; Nichia Corp. Japan) is mounted on an aluminum plate providing improved heat dissipation. The light emitted at a large solid angle (>45°) is collected by a high N.A. aspherical condenser lens (KPA022, Coherent Scientific, Australia, this product has been discontinued; however, the another lens with equivalent light collection power can be used, for example, the KPA040, f = 22 mm and D = 40 mm, http://www.newport.com) and passes via a UV excitation filter (U330 filter, Edmund Optics) and dichroic (FT395, >400 nm pass; Carl Zeiss, Australia) 45° turning-mirror to the microscope objective (×20, N.A. = 0.45; ×60, N.A. = 0.85). The fluorescence image collected by the objective is projected by the ×10 eyepiece 1 onto the focal plane (spot diameter ~1.5 mm for ×20 objective and ~1.0 mm for the ×60 objective), where a 1.0 mm-diameter fixed pinhole and the spinning optical chopper blade (C995 Optical Chopper, Terahertz Technologies, Inc., NY) are positioned. The fluorescence signal transmitted through the chopper during the signal collection window is then reimaged to the far field by eyepiece 2 to enable direct visual inspection by the eye. Alternatively, time-gated fluorescence images could be recorded by camera (Nikon DS-2Mv Color Digital Camera (1600 × 1200 pixels, Nikon Instruments Inc. USA)), and video data (live image frames) could be analyzed using imageJ software.

For the chopper itself, we chose a Model C995 Optical Chopper, Terahertz Technologies, Inc., NY, giving maximum rotation rate of 167 revolutions per second with a 30 slot, 1:1 duty ratio, and chopper blade of radius r = 42 mm giving 100 μs signal collection window at 5 kHz. For duty ratio of 3:1, the original chopper wheel was modified by removing every second blade, and for duty ratio 5:1, every second and third blades were removed (by laser-machining). At maximum rps, this gave a 300 μS signal collection window at 2.5 kHz and a 500 μs window at 1 kHz. For maximum chopper revolution rate (167 rps), we obtained open/close transition times as short as 16 μs for the ×20 objective and 11 μs for the ×60 objective (see Figure S1 in Supporting Information section S4). In the case of The TTL synchronization signal provided by the chopper, a module was used as the reference signal for the pulse synchronizer which generated a delayed signal to trigger the UV LED drive, delivering a fixed excitation pulse of 75 μs. The sample preparation information is described in Supporting Information S5 *Giardia Lamblia* Cysts and *Cryptosporidium Parvum* Oocysts Labeling and S6 Environmental Water Sample Preparation.

RESULTS AND DISCUSSION

To explore the optimized excitation and detection efficiencies, we first evaluate the performance of our prototype time-gated luminescence microscope by the FireRed 5.0 μm-diameter europium-doped calibration microspheres (Newport Instruments, San Diego, USA). Achieving the optimized conditions (see details in Supporting Information sections S1−S4), we use this TGL microscope for the real-time direct-visual inspection of Eu^{3+}-labeled *Giardia lamblia* cysts in water dirts and *Cryptosporidium parvum* oocysts in fruit juice concentrate. Signal-to-background ratio was enhanced typically by more than 1 order of magnitude.

In detail, the theoretical excitation efficiency for the UV LED-excited time-gated microscope described here was calculated in Supporting Information section S2 as ~3%. Referring to Supporting Information section S7 and Figure S2, for FireRed 5.0 μm-diameter europium-doped calibration microspheres, there was a linear relationship between the excitation power and time-gated luminescence up to the maximum LED power available. This suggests there is considerable scope for further improvement in luminescence intensity based on increased UV LED power. Referring also to Supporting Information section S8, we have also measured the time-gated luminescence emission collection efficiency (time-gated mode vs conventional mode for europium emission) for the current microscope as 72.1% for 3:1 (open vs shut) duty ratio.

The time-gated luminescence imagings of *Giardia lamblia* and *Cryptosporidium parvum* within water concentrates have been previously presented by our group.[42] This model has been established as one of the demonstration kits to evaluate our recent developments in both instrumentation and bioprobes.[2,22,23,30−32,34,43−48] Our previous time-gated luminescence bioimagings suffer from long exposure time and monochrome images by expensive setups. As one of the main advances achieved by this work, Figure 3A,B showed the recorded true-color images of a single *Giardia lamblia* cyst labeled by a BHHCT-europium complex within environmental water concentrate (dirt). In the absence of time-gated detection as in Figure 3A, the labeled target microorganism *Giardia lamblia* (6−9 μm in diameter) as well as other nontarget microorganisms and debris emit strongly across the full visible spectrum of colors under UV excitation making it extremely difficult to unambiguously identify the target. Applying time-gated detection (UV excitation pulse 75 μs, gate delay 5 μs, signal collection window 320 μs at 2.5 kHz cycling rate) as shown in Figure 3B, the background autofluorescence is substantially suppressed enabling the target microorganism *Giardia lamblia* to be clearly distinguished by the eye (both images were captured by 1 s camera exposure time). A video (Supporting Information) recorded the real-time process from the chopper switching-on until the moment when the excitation pulse and signal collection period were locked in antiphase for the microscope to operate in the time-gated luminescence mode.

The combination of temporal, spectral, intensity, and spatial resolutions, provided by true-color time-gated luminescence

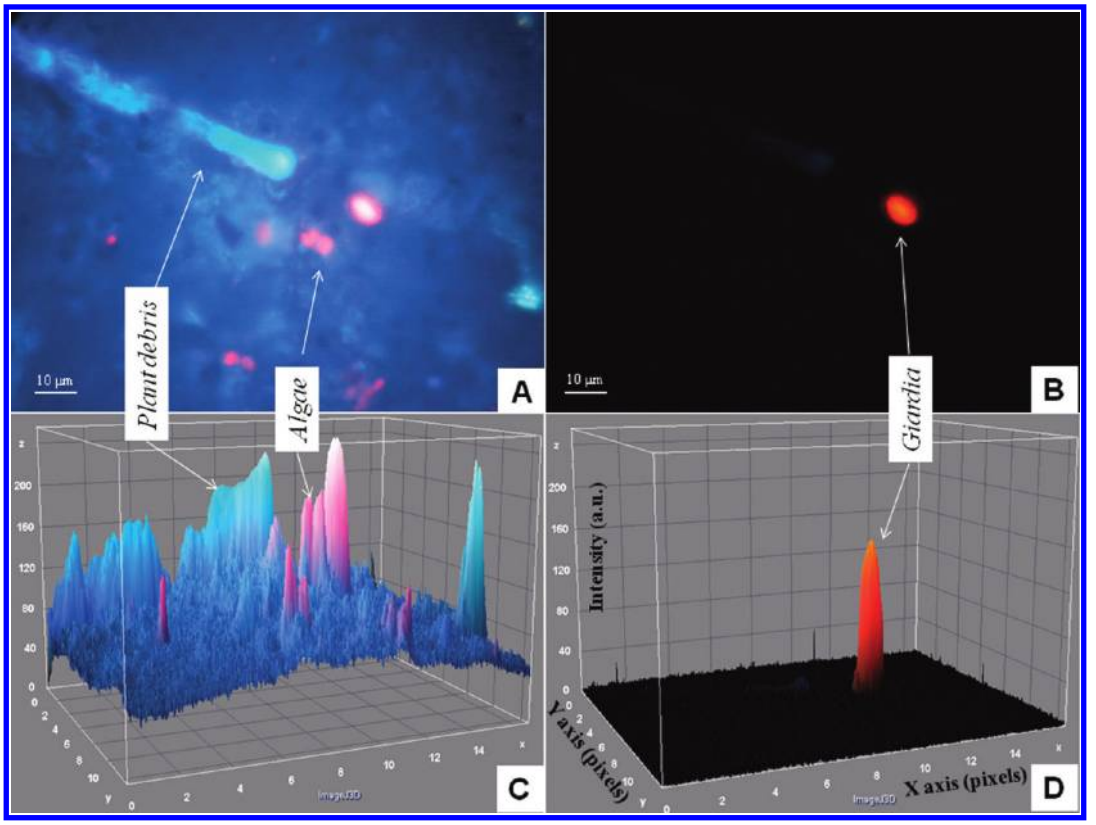

Figure 3. True-color images of a single *Giardia lamblia* cyst labeled by a BHHCT-europium complex within environmental water concentrate: (A) conventional fluorescence microscope image; (B) time-gated luminescence microscope image. (C and D) True-color time-gated luminescence bioimaging allows a 3D analysis of the time-gated luminescence images by a standard CCD camera and analysis using ImageJ software.

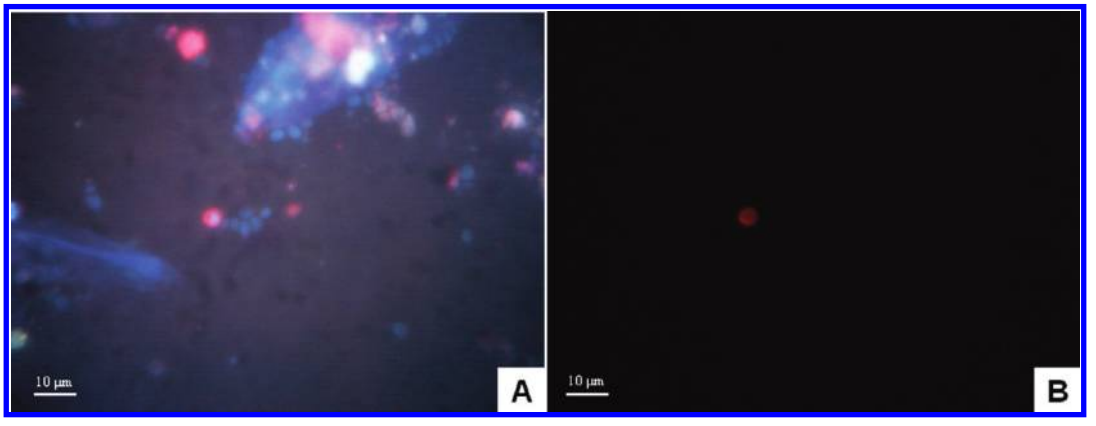

Figure 4. True-color images of a BHHCT-europium complex labeled *Cryptosporidium parvum* oocyst within fruit juice concentrate: (A) conventional fluorescence microscope image; (B) time-gated luminescence microscope image.

imaging recorded through a standard camera, allows for advanced data analysis as illustrated in Figure 3C,D, showing a 3-D dynamic analysis of the images of Figure 3A,B via the NIH ImageJ software. The signal to background ratio (measured by the ratio of luminescence intensity of *Giardia* vs autofluorescence signal from the highest nontarget peak) is seen to improve 18-fold (from 247/204 to 129/6) from conventional to time-gated mode of operation. We note that this is approximately a factor of 2 below the enhancement of signal-to-background ratio that we have achieved with fully electronic versions of TGL microscopes;[34,45] this is due to the comparatively slow gate closed/gate open transition time which can be achieved with fast choppers as compared to electronic switching of MCP- or gain-switched CCDs[34,45] as well as the rapid shut CCD camera by the analog method.[37]

As another demonstration to evaluate the current optimized setup, we applied the time-gated luminescence microscope to real-time direct-visual inspection of much smaller micro-organisms, *Cryptosporidium parvum* oocysts (~3 μm in diameter), in fruit juice concentrates as shown in Figure 4. Analysis of recorded image data using imageJ software shows the luminescence signal to autofluorescence background ratio (luminescence intensity of

Cryptosporidium vs red autofluorescence background intensity of juice debris) was enhanced by 12.8-fold (from 159/198 to 41/4).

CONCLUSION

Previous reports[36] of electronic time-gated luminescence bioimaging have demonstrated high-contrast imaging; however, these generally require long signal integration time (typically >30 s), and true-color spectral resolution is sacrificed through the necessity of the use of sensitive gateable monochrome cameras. In contrast, the simple optomechanical TGL microscope reported here has proved successful for direct visual observation (or recorded image using a standard color CCD camera) of time-gated lanthanide luminescence in an effectively background-free condition. We have demonstrated that a conventional fluorescence microscope can be modified at relatively low cost (<US $2000) with very limited structural change to the microscope. Use of a standard color CCD camera to record the time-gated images allows multidimensional image analysis using standard software packages. We envision this simple and practical method can have a large impact on lanthanide (as well as phosphorescent dye) based advanced biosensing areas. These might include continuous monitoring of biological cellular processes (e.g., cellular chemical sensing of pH, cations using lanthanide complexes as active sensors) in real time,[27,28,49] tissue imaging (time-resolved),[18] and lanthanide sensitized fluorescence resonance energy transfer (FRET) emission mapping (in which a long-lived chelate is used as energy transfer donor and a fluorophore with a lifetime in the nanosecond range as the acceptor[35]), as well as lifetime mapping.[50] Further instrumentation developments might take advantage of time-gated luminescence microscopy with multicolor labels and a range of available laser diodes as excitation sources.[6] We believe this simple technology represents a major opportunity to open up lanthanide-based biomedical and analytical diagnostics applications.

ASSOCIATED CONTENT

Supporting Information. Additional information as noted in text. This material is available free of charge via the Internet at http://pubs.acs.org.

AUTHOR INFORMATION

Corresponding Author
*E-mail: dayong.jin@mq.edu.au.

ACKNOWLEDGMENT

The authors wish to acknowledge Prof. Yuan's group at Dalian University of Technology for providing BHHCT chelates and Newport Instruments (San Diego, USA) for providing europium-doped FireRed calibration beads, as well as research funding from Australian Research Council (Discovery Project DP 1095465), Macquarie University Research Fellowship Scheme, and the ISAC (International Society for Advancement of Cytometry) scholar program.

REFERENCES

(1) Bajaj, S.; Welsh, J. B.; Leif, R. C.; Price, J. H. *Cytometry* **2000**, *39*, 285–294.
(2) Jin, D. Y.; Piper, J. A.; Leif, R. C.; Yang, S.; Ferrari, B. C.; Yuan, J. L.; Wang, G. L.; Vallarino, L. M.; Williams, J. W. *J. Biomed. Opt.* **2009**, 14.
(3) Weibel, N.; Charbonniere, L. J.; Guardigli, M.; Roda, A.; Ziessel, R. *J. Am. Chem. Soc.* **2004**, *126*, 4888–4896.
(4) Veal, D. A.; Deere, D.; Ferrari, B.; Piper, J.; Attfield, P. V. *J. Immunol. Methods* **2000**, *243*, 191–210.
(5) Yuan, J. L.; Wang, G. L. *TrAC, Trends Anal. Chem.* **2006**, *25*, 490–500.
(6) Bunzli, J. C. G. *Chem. Lett.* **2009**, *38*, 104–109.
(7) Soini, A. E.; Kuusisto, A.; Meltola, N. J.; Soini, E.; Seveus, L. *Microsc. Res. Tech.* **2003**, *62*, 396–407.
(8) Leif, R.; Clay, S. P.; Gratzner, H. G.; Haines, H. G.; Rao, K. V.; Vallarino, L. M. . *The Automation of Uterine Cancer Cytology*, Wied, G. L., Bahr, G. F., Bartels, P. H., Eds.; Tutorials of Cytology: Chicago, IL,1976, pp 313−344.
(9) Soini, A. E.; Hemmila, I. *Clin. Chem.* **1979**, *25*, 353–361.
(10) Siitari, H.; Hemmila, I.; Soini, E.; Lovgren, T.; Koistinen, V. *Nature* **1983**, *301*, 258–260.
(11) Soini, A. E.; Lovgren, T. *CRC Crit. Rev. Anal. Chem.* **1987**, *18*, 105–154.
(12) Hemmila, I.; Malminen, O.; Mikola, H.; Lovgren, T. *Clin. Chem.* **1988**, *34*, 2320–2322.
(13) Yuan, J. L.; Matsumoto, K. *J. Pharm. Biomed.* **1997**, *15*, 1397–1403.
(14) Yuan, J. L.; Matsumoto, K.; Kimura, H. *Anal. Chem.* **1998**, *70*, 596–601.
(15) Yuan, J. L.; Wang, G. L.; Majima, K.; Matsumoto, K. *Anal. Chem.* **2001**, *73*, 1869–1876.
(16) Templeton, E.; Wong, H.; Evangelista, R.; Granger, T.; Pollak, A. *Clin. Chem.* **1991**, *37*, 1506–1512.
(17) Seveus, L.; Vaisala, M.; Syrjanen, S.; Sandberg, M.; Kuusisto, A.; Harju, R.; Salo, J.; Hemmila, I.; Kojola, H.; Soini, E. *Cytometry* **1992**, *13*, 329–338.
(18) Bornhop, D. J.; Hubbard, D. S.; Houlne, M. P.; Adair, C.; Kiefer, G. E.; Pence, B. C.; Morgan, D. L. *Anal. Chem.* **1999**, *71*, 2607–2615.
(19) Hanaoka, K.; Kikuchi, K.; Kobayashi, S.; Nagano, T. *J. Am. Chem. Soc.* **2007**, *129*, 13502–13509.
(20) Gahlaut, N.; Miller, L. *Cytometry, Part A* **2010**, *77A*, 1113–1125.
(21) Fernández-Moreira, V.; Song, B.; Sivagnanam, V.; Chauvin, A.; Vandevyver, C.; Gijs, M.; Hemmilä, I.; Lehr, H.; Bünzli, J. *Analyst* **2010**, *135*, 42–52.
(22) Jin, D.; Connally, R.; Piper, J. *Cytometry, Part A* **2007**, *71A*, 783–796.
(23) Jin, D.; Connally, R.; Piper, J. *Cytometry, Part A* **2007**, *71A*, 797–808.
(24) Petoud, S.; Cohen, S. M.; Bunzli, J. C. G.; Raymond, K. N. *J. Am. Chem. Soc.* **2003**, *125*, 13324–13325.
(25) Deiters, E.; Song, B.; Chauvin, A. S.; Vandevyver, C. D. B.; Gumy, F.; Bunzli, J. C. G. *Chem.—Eur. J.* **2009**, *15*, 885–900.
(26) Song, B.; Wang, G. L.; Tan, M. Q.; Yuan, J. L. *J. Am. Chem. Soc.* **2006**, *128*, 13442–13450.
(27) Thibon, A.; Pierre, V. C. *J. Am. Chem. Soc.* **2009**, *131*, 434–335.
(28) Thibon, A.; Pierre, V. C. *Anal. Bioanal. Chem.* **2009**, *394*, 107–120.
(29) Makhluf, S. B. D.; Arnon, R.; Patra, C. R.; Mukhopadhyay, D.; Gedanken, A.; Mukherjee, P.; Breitbart, H. *J. Phys. Chem. C* **2008**, *112*, 12801–12807.
(30) Wu, J.; Ye, Z. Q.; Wang, G. L.; Jin, D. Y.; Yuan, J. L.; Guan, Y. F.; Piper, J. *J. Mater. Chem.* **2009**, *19*, 1258–1264.
(31) Wu, J.; Wang, G. L.; Jin, D. Y.; Yuan, J. L.; Guan, Y. F.; Piper, J. *Chem. Commun.* **2008**, 365–367.
(32) Song, C. H.; Ye, Z. Q.; Wang, G. L.; Jin, D. Y.; Yuan, J. L.; Guan, Y. F.; Piper, J. *Talanta* **2009**, *79*, 103–108.
(33) Harma, H.; Soukka, T.; Lovgren, T. *Clin. Chem.* **2001**, *47* 561–568.
(34) Connally, R.; Piper, J. *J. Biomed. Opt.* **2008**, *13* (3), 034022.

(35) Vereb, G.; Jares-Erijman, E.; Selvin, P. R.; Jovin, T. M. *Biophys. J.* **1998**, *74*, 2210–2222.
(36) Connally, R.; Piper, J. *Ann. N.Y. Acad. Sci.* **2008**, *1130*, 106–116.
(37) Leif, R.; Yang, S. *Proceeding of The International Society for Optical Engineering (SPIE)*, Vol. 7568, San Francisco, California, USA, 2010; 75681A.
(38) Jin, D.; Piper, J.; Yuan, J.; Leif, R. *Proceeding of The International Society for Optical Engineering (SPIE)*, Vol. 7568, San Francisco, California, USA, The International Socity for Optical Engineering (SPIE): Bellingham, WA, 2010; 756819.
(39) Li, Q. Y.; Dasgupta, P. K.; Temkin, H. *Anal. Chim. Acta* **2008**, *616*, 63–68.
(40) Kimura, H.; Mukaida, M.; Watanabe, M.; Hashino, K.; Nishioka, T.; Tomino, Y.; Yoshida, K. I.; Matsumoto, K. *Anal. Biochem.* **2008**, *372*, 119–121.
(41) Hashino, K.; Ikawa, K.; Ito, M.; Hosoya, C.; Nishioka, T.; Makiuchi, M.; Matsumoto, K. *Anal. Biochem.* **2007**, *364*, 89–91.
(42) Connally, R.; Veal, D.; Piper, J. *FEMS Microbiol. Ecol.* **2002**, *41*, 239–245.
(43) Connally, R.; Veal, D.; Piper, J. *J. Biomed. Opt.* **2004**, *9*, 725–734.
(44) Connally, R.; Veal, D.; Piper, J. *Microsc. Res. Tech.* **2004**, *64*, 312–322.
(45) Connally, R.; Jin, D.; Piper, J. *Cytometry, Part A* **2006**, *69A*, 1020–1027.
(46) Jiang, H. F.; Wang, G. L.; Zhang, W. Z.; Liu, X. Y.; Ye, Z. Q.; Jin, D. Y.; Yuan, J. L.; Liu, Z. G. *J. Fluoresc.* **2010**, *20*, 321–328.
(47) Jiang, L. N.; Wu, J.; Wang, G. L.; Ye, Z. Q.; Zhang, W. Z.; Jin, D. Y.; Yuan, J. L.; Piper, J. *Anal. Chem.* **2010**, *82*, 2529–2535.
(48) Deng, W.; Jin, D.; Drozdowicz-Tomsia, K.; Yuan, J.; Goldys, E. *Langmuir* **2010**, *26*, 10036–10043.
(49) Botchway, S. W.; Charnley, M.; Haycock, J. W.; Parker, A. W.; Rochester, D. L.; Weinstein, J. A.; Williams, J. A. G. *P. Natl. Acad. Sci. U.S. A.* **2008**, *105*, 16071–16076.
(50) Beeby, A.; Botchway, S. W.; Clarkson, I. M.; Faulkner, S.; Parker, A. W.; Parker, D.; Williams, J. A. G. *J. Photochem. Photobiol., B* **2000**, *57*, 83–89.
(51) Jin, D.; Connally, R.; Piper, J. *J. Phys. D. Appl. Phys.* **2006**, *39*, 461–465.